

Journal of Materials Chemistry C

Accepted Manuscript



This is an *Accepted Manuscript*, which has been through the Royal Society of Chemistry peer review process and has been accepted for publication.

Accepted Manuscripts are published online shortly after acceptance, before technical editing, formatting and proof reading. Using this free service, authors can make their results available to the community, in citable form, before we publish the edited article. We will replace this *Accepted Manuscript* with the edited and formatted *Advance Article* as soon as it is available.

You can find more information about *Accepted Manuscripts* in the [Information for Authors](#).

Please note that technical editing may introduce minor changes to the text and/or graphics, which may alter content. The journal's standard [Terms & Conditions](#) and the [Ethical guidelines](#) still apply. In no event shall the Royal Society of Chemistry be held responsible for any errors or omissions in this *Accepted Manuscript* or any consequences arising from the use of any information it contains.

Solution-assembled nanowires for high performance flexible and transparent solar-blind photodetectors

Cite this: DOI: 10.1039/x0xx00000x

Jiangxin Wang,^a Chaoyi Yan,^a Meng-Fang Lin,^b Kazuhito Tsukagoshi^b and Pooi See Lee^{*a}

Received 00th January 2014,
Accepted 00th January 2014

DOI: 10.1039/x0xx00000x

www.rsc.org/

Solar-blind photodetectors based on Zn₂GeO₄ (ZGO) nanowires (NWs) with high transparency and good flexibility were successfully fabricated on polyethylene terephthalate (PET) substrate using a facile all solution-processible method. The electrodes and functional channels are constructed with silver NWs (AgNWs) and ZGO NWs respectively, using spray coating method. The spray-coated all-NW device exhibited high transparency, good mechanical bending stability, high photoresponse, and short cutoff wavelength. The Schottky barrier between the Ag-ZGO NWs together with the junction barrier between interconnecting ZGO NWs contributed to high photoresponse and improved switching time in the devices. We propose that the unique energy band structure of the ZGO NW networks provides additional mechanism to further reduce the cutoff wavelength in the solar-blind photodetectors.

Introduction

Flexible and transparent electronics are of great interest for many emerging applications.¹⁻⁴ The capability to fabricate optically transparent and mechanically flexible electronics paves the way to the next-generation “see-through” and conformable devices. Solar-blind photodetectors which detect light in the spectra range of 190-280 nm have important applications in biological threat detection, missile tracking, flame detection, and ozone hole sensing etc.⁵⁻⁷ Flexible and meanwhile transparent solar-blind photodetectors enable the integration of wearable monitoring and sensing systems on top of other devices without affecting visibility of the below devices. NWs are promising building blocks for these devices. They possess inherent mechanical flexibility and can be easily coated onto arbitrary substrates by inkjet printing, spin coating, drop casting or spray coating methods etc, meeting the prospects of large-area processability and low-temperature compatibility with most of the flexible substrates. The prototypical indium tin oxide (ITO) is normally used as the transparent electrodes in transparent photodetectors while nanowires were used as the sensing materials.^{8,9} Limited by the brittle nature and high temperature deposition process of the ITO electrode, the advantages of NW in large bending strain compliance and low-temperature processability could not be

fully utilized. On the other hand, percolating metal NWs have recently attracted great interest for electrode applications and been demonstrated to be promising alternatives with their good conductivity, solution processability, high transparency and flexibility.¹⁰⁻¹⁵ Among these materials, AgNWs film is an outstanding candidate which offers good conductivity and transparency (~10 Ω/sq with 90% transmittance).

Semiconductor nanowires have been extensively studied for applications in photodetectors.¹⁶⁻²³ It is widely recognized that the 1D nanostructure contributes to high photosensitivity due to the large surface-to-volume ratio which prolongs lifetime of the photo-generated carriers with appreciable band bending on the nanowire surface. It is demonstrated in this report that the unique property in NWs not only provides high photosensitivity to the NW photodetectors, it can also introduce additional mechanism to reduce photoresponse time and the cutoff wavelength of the photodetectors while assembled into the network structure. Wide-bandgap semiconductor NWs are promising materials for solar-blind photodetectors. Their large bandgaps minimize the chance of false detection and reduce high background under infrared or visible light, eliminating the use of expensive and bulky optical filters. Recently, β-Ga₂O₃ nanostructures,^{24,25} In₂Ge₂O₇ nanowires,²⁶ and Zn₂GeO₄ NWs^{27,28} have been used as solar-blind light detection

materials. However, these devices still showed certain photoresponse to the incident light with wavelength longer than 280 nm. Moreover, the fabrication approaches in these reports typically involved complicated lithography fabrication procedures. Efficient large-scale device fabrication for flexible and transparent NW solar-blind photodetection is still lacking. Hereby, we report that with the use of a simple solution-assembly method, high performance flexible and transparent solar-blind photodetectors can be fabricated. The method helps to tackle the aforementioned difficulties while full advantages of NWs in their large mechanical compliance and low temperature processability can be harvested.

Experimental

Device fabrication

ZGO NWs were grown on Si substrates by a chemical vapor deposition (CVD) method.²⁹ The NWs were removed from the substrates and dispersed in isopropyl alcohol (IPA) at a concentration of ~0.1 mg/ml with sonication for 15 min. The AgNWs solution was purchased from Seashell Technology with diameters of 120-150 nm and lengths of 20-50 μm . The concentration was diluted to 0.5 mg/ml in IPA before use. Fig. 1a illustrates the fabrication procedures of the flexible and transparent UV photodetectors. First, the ZGO NW solution was spray-coated onto the PET substrate through a shadow mask, forming the light detection channels. Second, AgNWs were coated analogously through another shadow mask, forming the transparent and conductive percolating AgNW

network electrodes. The resultant photodetectors had a channel length of 0.15 mm and channel width of 1.2 mm. Two ml of ZGO NW solution and 1 ml of AgNW solution were used to coat onto a substrate area of 2x2 cm. Due to the fast evaporation rate of IPA, no substrate heating is required during the spray-coating process.

Characterization

SEM images of the samples were taken with a field-emission SEM (FE-SEM, JSM 7600F). The X-ray diffraction patterns were measured on a Shimadzu XRD-6000 instrument with Cu K α radiation. The transmittance spectra were measured by a Shimadzu spectrometer (UV-2550). Electrical properties of the photodetector were characterized by a Keithley 4200-SCS parameter analyzer equipped with remote PreAmp models to enable low current measurement. Photoresponse of the device under different wavelengths were measured using a wavelength tunable monochromatic light source, which included a 150 W xenon lamp and an Omni λ -series monochromator with output bandwidth of 0.2 nm. The bending test was carried out on a home-made translation stage. The photodetector performance was measured when the stage compressed the devices to different bending angles.

Result and Discussion

Fig. 1b shows a schematic image of the flexible NW photodetector. The highly conductive AgNW networks construct the transparent electrodes. The ZGO interconnecting NW networks were homogeneously dispersed on the substrate, locating below the AgNW electrodes as the solar-blind light detection channels. Five by five photodetector arrays were fabricated on a PET substrate. The photodetector shows excellent transparency with the letters clearly seen under the device, as shown in Fig. 1c. The photograph in Fig. 1d demonstrates a device under bending. The photodetector can be repetitively bended to an angle of 90° and released. No peeling or deformation of the device structures were observed after the bending. The haze appearance in the device is due to light scattering by the NW films.

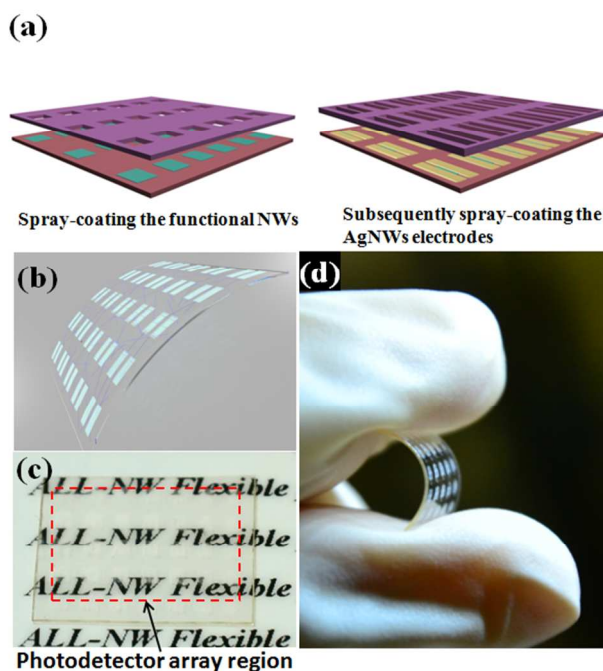


Fig. 1 (a) Schematic images of the device fabrication procedures. (b) A schematic image of the transparent and flexible photodetectors. (c-d) Photographs showing good transparency and flexibility of the device.

Morphology of the AgNWs and ZGO NWs were presented in Fig. 2a, b respectively. Large amount of ZGO NWs on the silicon substrate could be synthesized by the CVD method (~10 mg nanowires on a 1x1.5 cm substrate). The nanowires were quite homogenous and possessed a high aspect ratio with the diameter of ~100 nm and length typically around 100 μm . Fig. 2c is the SEM imaging of the photodetector at the channel/electrode overlap region. The region on the right side of the dashed line contains pure Ag NWs while the left region is the overlap between the electrode and detection channel which contains AgNWs and ZGO NWs. The two types of NWs form percolating NW networks, establishing good connection between the device's electrode and channel. The XRD patterns in Fig. 2d show that the NWs have a pure rhombohedral crystal

phase (JCPDS: 011-0687, $a=14.231 \text{ \AA}$, $b=9.53 \text{ \AA}$). The high crystallinity nature of the ZGO NWs eliminates our concern of impurity which may affect the device performance. The ultra-high photoresponse behavior of the device can also be partially attributed to the high purity and good crystallinity of the ZGO NWs synthesized by the CVD method.

The device achieved a high transparency of $\sim 80\%$ transmittance in the visible light range with transmittance of the pure PET substrate at 90%, as shown in Fig. 3a. Transmittance of the devices can be further improved by using PET substrate with higher transparency. Due to light scattering by the NW networks, the device transmittance value might be underestimated as the ultraviolet-visible spectroscopy in our experiment is not capable of measuring the scattered light transmitted through the device.³⁰ Fig. 3b illustrates the I-V curve of the devices under 250 nm UV light illumination and dark condition. The asymmetric behavior in the I-V characteristic was attributed to the different contact conditions at the two sides of the electrodes.^{27,28} The nonlinear I-V curve indicates the existence of energy barriers in the device. Dark current of the device is around 10 fA at 10 V bias. The extremely small dark current can be attributed to the low carrier intensity ($1.78 \times 10^{17} \text{ cm}^{-3}$, calculated by Liu et al.³¹) in the intrinsic ZGO NWs. In addition, both the AgNW-ZGO NW Schottky barrier and ZGO NW-ZGO NW junction barrier contributed to further suppress of the dark current. The photocurrent of the device significantly increases to 30 pA while it is illuminated with UV light at 250 nm ($\sim 0.2 \text{ mW/cm}^2$), giving an on/off ratio of 3000. The on/off ratio is much higher compared to reported UV photodetectors using ZGO NWs as the light detection materials (typically dozens of times^{28,31-33}) and closed to the best reported result which showed a on/off ratio of a few thousands of times on devices fabricated by an elaborate e-beam lithography method.²⁷ The photocurrent jumps to the maximum value immediately after the UV light is

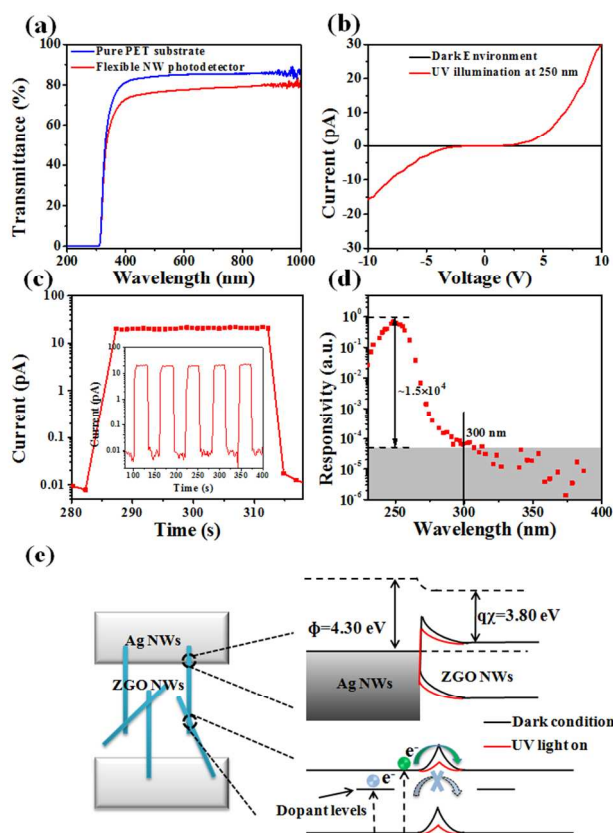


Fig. 3 (a) Transmittance spectra of the pure PET substrate and the flexible NW photodetector. (b) I-V curves of the photodetector under dark and illumination conditions. (c) Photoresponse behavior of the devices. Inset shows the device performance with periodical on/off (30 s/30 s) cycles. (d) Responsivity of the devices biased with 10 V at different wavelengths. (e) Schematic of the energy band structures in the NW network devices with and without light illumination. The energy band structures (both at dark and illumination conditions) are given in short-circuit.

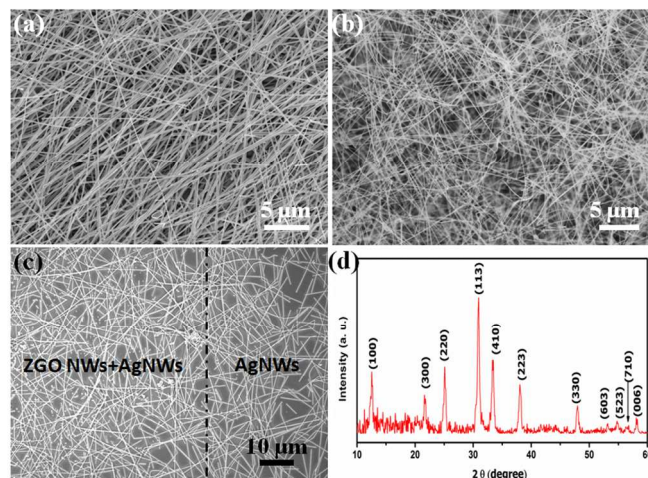


Fig. 2 Top SEM images of (a) AgNWs, (b) ZGO NWs, and (c) ZGO NWs and Ag NWs interface region in the photodetector device. (d) XRD pattern of the ZGO NWs.

on, as shown in Fig. 3c. The device recovers to the dark current promptly after the UV light is off. The respond time and reset time are below 5 s and 2.6 s respectively. It should be noted that the switching time was limited by the fastest measurement time of the equipment which was prolonged by the extremely low dark current in the device. The respond time is faster compared to the reported single ZGO NW photodetector (12 s).²⁷ The improved respond time and high photoresponse are attributed to the Schottky barriers and NW junction barriers between the NW networks, as interpreted in Fig. 3e. The work function of AgNWs is around 4.3 eV while the conduction band of ZGO NWs locates at around 3.8 eV. Mismatch in the energy levels leads to Schottky barrier formation at the AgNW-ZGO NW interface. Band bending at the ZGO NWs surface will also generate energy barriers at the ZGO NW junctions. It is understood that under light illumination, the Schottky barrier height will be lowered and its width will be narrowed.³⁴⁻³⁶ Similar effects were also observed on the ZGO NW junction barriers in the network structure.²⁸ Modulation of the barrier

height and width under light illumination is the dominant mechanism dictating the photocurrent transport behavior in the device. The carrier transport is mainly restricted at the energy barriers. The reduction of barrier height and width will lead to gating effect which significantly increases the photocurrent. As the modulation only takes place at the interface instead of the whole NW surface, it provides a faster switching mechanism for the photodetectors.³⁵

Responsivity of the device over different wavelength was measured by scanning the light generated from a xenon light source from 220 nm to 400 nm, as shown in Fig. 3d. The device exhibited increasing respond to the incident light when the wavelength is close to 268 nm (the bandgap of ZGO NWs, ~ 4.6 eV). The photoresponse continued to increase when the wavelength was reduced and reached the maximum value at 250 nm. The cutoff wavelength of the device was ~ 300 nm. The solar blind (250 nm)-UV (300 nm) rejection ratio was around 1.5×10^4 , comparable to the previous report on single ZGO NW photodetector with a rejection ratio of around 1×10^4 at the wavelengths of 245 nm-380 nm.²⁷ However, the single ZGO NW photodetector showed response to the light illumination until the wavelength increased above 380 nm. Photoresponse of the device in the long wavelength can be attributed to the unintentional doping of the NWs, such as oxygen vacancies and zinc interstitial²⁹ formed during the CVD synthesis process. Electrons can be excited into the shallow dopant levels under the conduction band by the low-energy photons and contribute to the photocurrent.^{37,38} However, the energy of these electrons is not sufficient to effectively lower and narrow the energy barrier at the ZGO NW-NW junctions. Existence of the junction barrier provides an addition "filter" to prohibit the transport of electrons excited by the low-energy photons. Consequently, the cutoff wavelength of the ZGO NW network photodetector was further reduced to around 300 nm, making it an ideal candidate for solar-blind detection.

Performance of the NW photodetector was tested under different bending angles as presented in Fig. 4a. The bending angle (2θ) is defined in Fig. 4b inset. A decrease of $\sim 12\%$ in the photocurrent was observed at the bending angle of 90° which might be attributed to the tensile strain in the device channels under the bending states. The photodetector possessed good cycling stability in the bending and relaxing test. As shown in Fig. 4b, after bending for 50, 100 and 150 cycles with a bending angle of 90° , dark current of the device remained almost constant after the bending cycles. The photocurrent showed slightly decrease from 16.6 pA to 16.3 pA after 50 bending cycles and increases again to 16.4 pA after 150 bending cycles. The small photocurrent decrease during the initial bending cycles was probably due to the sliding of NWs and losing interconnection in the NW networks. The sliding might be minor and the interconnection could be occasionally established again after the bending, as shown at the 150 cycles with some increase in the photocurrent. Consequently, small photocurrent fluctuation was observed during the bending test. In brief, the photodetector showed excellent flexibility and stability which was comparable to previous works on flexible photodetectors.³⁹⁻⁴¹ The results suggest that the photodetectors are encouraging for application in flexible and transparent solar-blind detection.

Conclusion

In conclusion, flexible and transparent photodetectors have been successfully fabricated based on an All-NW device configuration. The device exhibited good transparency of around 80% transmittance in the visible light range and demonstrated high flexibility and stability. The ZGO NWs used for the device fabrication had high purity and good crystallinity which contributed to the huge photoresponse of the device. The photodetectors have a large on/off ratio with the photocurrent

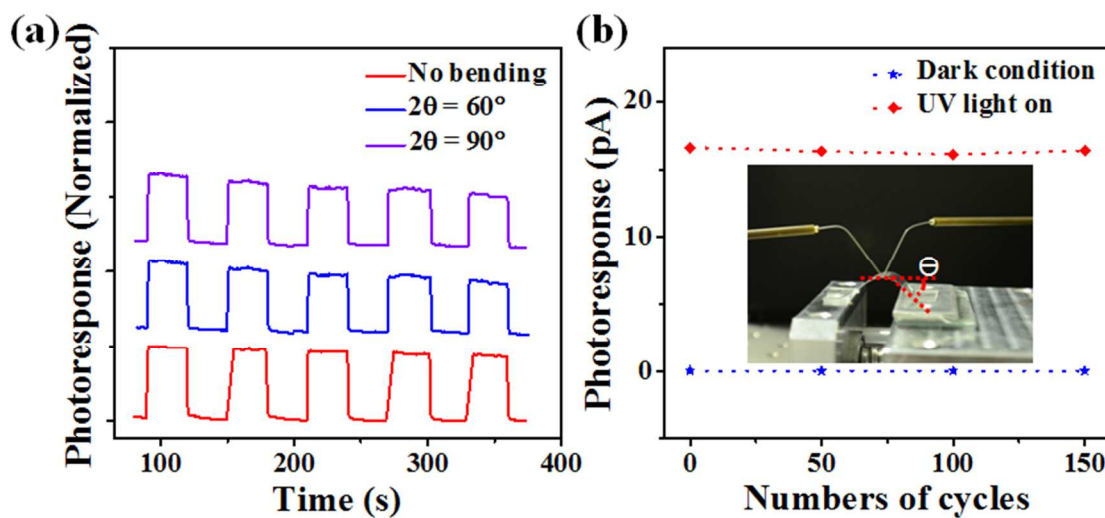


Fig. 4 (a) Performance of the UV-photodetector under bending angles of 0° , 60° and 90° . (b) Photoresponse of the device after different bending cycles in the relaxed state.

reaching 3000 times of the dark current. The network structure in the devices established Schottky barriers between the Ag-ZGO NWs and the NW-NW junction barriers between the interconnected ZGO NWs. These energy barriers enable the improved switching behavior of the photodetectors. The NW-NW junction barriers in the ZGO NWs also help to reduce the cutoff wavelength of the solar-blind detector. The solution processible method developed here is simple and facile which can be easily applied to other flexible and transparent device fabrication.

Acknowledgements

This work was supported in part by the joint program between Singapore and Japan supported by the Centre of Excellence for Silicon Technologies (Si-CoE) grant and Japan Society for the Promotion of Science (JSPS).

Notes and references

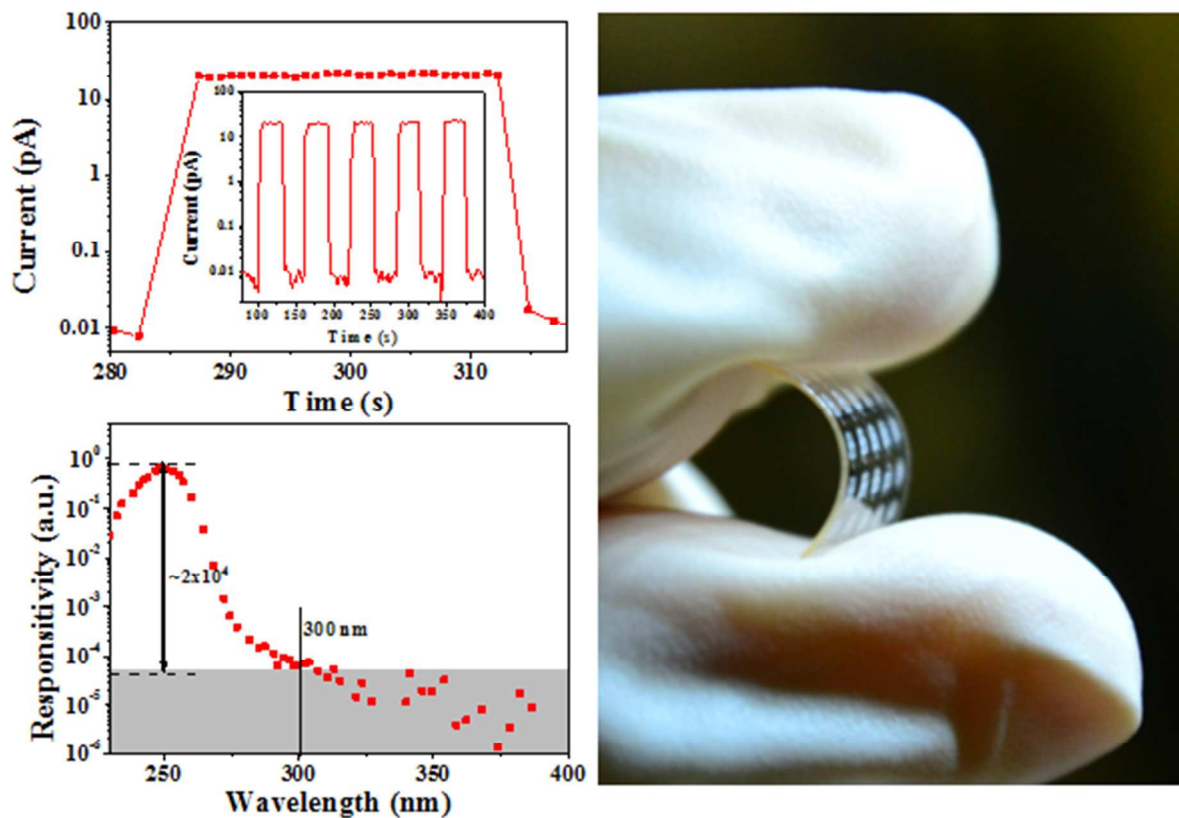
^a School of Materials Science and Engineering 50 Nanyang Avenue, Nanyang Technological University, Singapore 639798.

^b International Center for Materials Nanoarchitectonics (WPI-MANA), National Institute for Materials Science (NIMS), Tsukuba, Ibaraki 305-0044, Japan.

- K. Nomura, H. Ohta, A. Takagi, T. Kamiya, M. Hirano and H. Hosono, *Nature*, 2004, **432**, 488.
- T. Georgiou, R. Jalil, B. D. Belle, L. Britnell, R. V. Gorbachev, S. V. Morozov, Y. J. Kim, A. Gholinia, S. J. Haigh, O. Makarovskiy, L. Eaves, L. A. Ponomarenko, A. K. Geim, K. S. Novoselov and A. Mishchenko, *Nat. Nanotechnol.*, 2013, **8**, 100.
- P. C. Chen, G. Shen, S. Sukcharoenchoke and C. Zhou, *Appl. Phys. Lett.*, 2009, **94**, 043113.
- J. L. Zhang, C. Wang and C. W. Zhou, *ACS Nano*, 2012, **6**, 7412.
- M. Razeghi, *Proceedings of the IEEE*, 2002, **90**, 1006.
- A. A. Hussain, A. R. Pal and D. S. Patil, *Appl. Phys. Lett.*, 2014, **104**, 193301.
- Y. N. Hou, Z. X. Mei, Z. L. Liu, T. C. Zhang and X. L. Du, *Appl. Phys. Lett.*, 2011, **98**, 103506.
- W. Tian, T. Y. Zhai, C. Zhang, S. L. Li, X. Wang, F. Liu, D. Q. Liu, X. K. Cai, K. Tsukagoshi, D. Golberg and Y. Bando, *Adv. Mater.*, 2013, **25**, 4625.
- X. Liu, L. Jiang, X. Zou, X. Xiao, S. Guo, C. Jiang, X. Liu, Z. Fan, W. Hu, X. Chen, W. Lu, W. Hu and L. Liao, *Adv. Mater.*, 2014, **26**, 2919.
- M. S. Lee, K. Lee, S. Y. Kim, H. Lee, J. Park, K. H. Choi, H. K. Kim, D. G. Kim, D. Y. Lee, S. Nam and J. U. Park, *Nano Lett.*, 2013, **13**, 2814.
- A. R. Madaria, A. Kumar, F. N. Ishikawa and C. Zhou, *Nano Research*, 2010, **3**, 564.
- S. De, T. M. Higgins, P. E. Lyons, E. M. Doherty, P. N. Nirmalraj, W. J. Blau, J. J. Boland and J. N. Coleman, *ACS Nano*, 2009, **3**, 1767.
- E. C. Garnett, W. S. Cai, J. J. Cha, F. Mahmood, S. T. Connor, M. G. Christoforo, Y. Cui, M. D. McGehee and M. L. Brongersma, *Nat. Mater.*, 2012, **11**, 241.
- H. Wu, L. Hu, M. W. Rowell, D. Kong, J. J. Cha, J. R. McDonough, J. Zhu, Y. Yang, M. D. McGehee and Y. Cui, *Nano Lett.*, 2010, **10**, 4242.
- J. V. van de Groep, P. Spinelli and A. Polman, *Nano Lett.*, 2012, **12**, 3138.
- L. F. Hu, J. Yan, M. Y. Liao, L. M. Wu and X. S. Fang, *Small*, 2011, **7**, 1012.
- C. Y. Yan and P. S. Lee, *Science of Advanced Materials*, 2012, **4**, 241.
- C. Soci, A. Zhang, X. Y. Bao, H. Kim, Y. Lo and D. L. Wang, *J. Nanosci. Nanotechnol.*, 2010, **10**, 1430.
- C. Yan, J. Wang, X. Wang, W. Kang, M. Cui, C. Y. Foo and P. S. Lee, *Adv. Mater.*, 2013, **26**, 943.
- H. Kind, H. Q. Yan, B. Messer, M. Law and P. D. Yang, *Adv. Mater.*, 2002, **14**, 158.
- C. Soci, A. Zhang, B. Xiang, S. A. Dayeh, D. P. R. Aplin, J. Park, X. Y. Bao, Y. H. Lo and D. Wang, *Nano Lett.*, 2007, **7**, 1003.
- J. J. Wang, F. F. Cao, L. Jiang, Y. G. Guo, W. P. Hu and L. J. Wan, *J. Am. Chem. Soc.*, 2009, **131**, 15602.
- J. Wang, C. Yan, W. Kang and P. S. Lee, *Nanoscale*, 2014, **6**, 10734.
- R. Zou, Z. Zhang, Q. Liu, J. Hu, L. Sang, M. Liao and W. Zhang, *Small*, 2014, **10**, 1848.
- L. Li, E. Auer, M. Y. Liao, X. S. Fang, T. Y. Zhai, U. K. Gautam, A. Lugstein, Y. Koide, Y. Bando and D. Golberg, *Nanoscale*, 2011, **3**, 1120.
- L. Li, P. S. Lee, C. Yan, T. Zhai, X. Fang, M. Liao, Y. Koide, Y. Bando and D. Golberg, *Adv. Mater.*, 2010, **22**, 5145.
- C. Li, Y. Bando, M. Y. Liao, Y. Koide and D. Golberg, *Appl. Phys. Lett.*, 2010, **97**, 161102.
- C. Yan, N. Singh and P. S. Lee, *Appl. Phys. Lett.*, 2010, **96**, 0531081.
- J. X. Wang, C. Y. Yan, S. Magdassi and P. S. Lee, *ACS Appl. Mater. Interfaces*, 2013, **5**, 6793.
- L. Hu, H. S. Kim, J.-Y. Lee, P. Peumans and Y. Cui, *ACS Nano*, 2010, **4**, 2955.
- Z. Liu, B. Liang, G. Chen, G. Yu, Z. Xie, L. Gao, D. Chen and G. Shen, *J. Mater. Chem. C*, 2013, **1**, 131.
- Z. Liu, H. T. Huang, B. Liang, X. F. Wang, Z. R. Wang, D. Chen and G. Z. Shen, *Opt. Express*, 2012, **20**, 2982.
- C. H. Liao, C. W. Huang, J. Y. Chen, C. H. Chiu, T. C. Tsai, K. C. Lu, M. Y. Lu and W. W. Wu, *J. Phys. Chem. C*, 2014, **118**, 8194.
- T. Y. Wei, C. T. Huang, B. J. Hansen, Y. F. Lin, L. J. Chen, S. Y. Lu and Z. L. Wang, *Appl. Phys. Lett.*, 2010, **96**, 013508.
- Y. F. Hu, J. Zhou, P. H. Yeh, Z. Li, T. Y. Wei and Z. L. Wang, *Adv. Mater.*, 2010, **22**, 3327.
- J. Zhou, Y. D. Gu, Y. F. Hu, W. J. Mai, P. H. Yeh, G. Bao, A. K. Sood, D. L. Polla and Z. L. Wang, *Appl. Phys. Lett.*, 2009, **94**, 191103.
- D. Walker, E. Monroy, P. Kung, J. Wu, M. Hamilton, F. J. Sanchez, J. Diaz and M. Razeghi, *Appl. Phys. Lett.*, 1999, **74**, 762.
- J. Tang, G. Konstantatos, S. Hinds, S. Myrskog, A. G. Pattantyus-Abraham, J. Clifford and E. H. Sargent, *ACS Nano*, 2008, **3**, 331.
- L. B. Luo, X. B. Yang, F. X. Liang, J. S. Jie, Q. Li, Z. F. Zhu, C. Y. Wu, Y. Q. Yu and L. Wang, *CrystEngComm*, 2012, **14**, 1942.
- B. Aksoy, S. Coskun, S. Kucukyildiz and H. E. Unalan, *Nanotechnology*, 2012, **23**, 325202.

- 41 G. Yu, B. Liang, H. T. Huang, G. Chen, Z. Liu, D. Chen and G. Z. Shen, *Nanotechnology*, 2013, **24**, 095703.

Table of Content Graphic:



An All-NW ultraviolet photodetector with high photoresponse and improved switching time was fabricated by a solution assembly method.